Available online at www.sciencedirect.com
SCIENCE DIRECT®
Coastal Engineering 48 (2003) 139–149
Coastal Engineering
An International Journal for Coastal, Harbour and Offshore Engineers
www.elsevier.com/locate/coastaleng

Calibration and verification of a parametric wave model on barred beaches

B.G. Ruessink[a,*], D.J.R. Walstra[a], H.N. Southgate

[a] WL|Delft Hydraulics, Marine and Coastal Management, P.O. Box 177, 2600 MH Delft, The Netherlands

Received 31 May 2002; accepted 29 January 2003

Abstract

Since its introduction in 1978, the Battjes and Janssen model has proven to be a popular framework for estimating the cross-shore root-mean-square wave height H_{rms} transformation of random breaking waves in shallow water. Previous model tests have shown that wave heights in the bar trough of single bar systems and in the inner troughs of multiple bar systems are overpredicted by up to 60% when standard settings for the free model parameter γ (a wave height-to-depth ratio) are used. In this paper, a new functional form for γ is derived empirically by an inverse modelling of γ from a high-resolution (in the cross-shore) 300-h H_{rms} data set collected at Duck, NC, USA. We find that, in contrast to the standard setting, γ is not cross-shore constant, but depends systematically on the product of the local wavenumber k and water depth h. Model verification with other data at Duck, and data collected at Egmond and Terschelling (Netherlands), spanning a total of about 1600 h, shows that cross-shore H_{rms} profiles modelled with the locally varying γ are indeed in better agreement with measurements than model predictions using the cross-shore constant γ. In particular, model accuracy in inner bar troughs increases by up to 80%. Additional verifications with data collected on planar laboratory beaches show the new functional form of γ to be applicable to non-barred beaches as well. Our optimum γ cannot be compared directly to field and laboratory measurements of height-to-depth ratios and we do not know of a physical mechanism why γ should depend positively on kh.

Keywords: Wave breaking; Inverse modelling; Height-to-depth ratio; Sandbars

1. Introduction

In 1978, Battjes and Janssen presented a nowadays commonly applied model to estimate the cross-shore transformation of random breaking waves in shallow water. The model is a parametric model based on the wave energy balance, transforming a single representative wave height (the root-mean-square wave height, H_{rms}) with a constant period (the peak period T_{p}) and a representative wave angle (the peak or (energy-weighted) mean direction $\bar{\theta}$) through the surf zone. The breaking-induced dissipation is computed as the product of energy dissipation S in a single breaking wave and the probability of occurrence of breaking Q, where Battjes and Janssen (1978) described S on the basis of a bore-type dissipation model and adopted a clipped-Rayleigh probability density function (pdf) to estimate Q. The only free model parameter, γ, indi-

* Corresponding author. Now at Department of Physical Geography, Institute for Marine and Atmospheric Research Utrecht, Utrecht University, P.O. Box 80115, 3508 TC Utrecht, The Netherlands. Tel.: +31-30-2532405; fax: +31-30-2531145.

E-mail address: g.ruessink@geog.uu.nl (B.G. Ruessink).

0378-3839/03/$ - see front matter © 2003 Elsevier Science B.V. All rights reserved.
doi:10.1016/S0378-3839(03)00023-1

cates a breaker height-to-depth ratio. Using mainly small-scale laboratory data, Battjes and Stive (1985) determined that γ, assumed to be cross-shore constant, depends weakly on the deep-water wave steepness s_d as

$$\gamma = 0.5 + 0.4\tanh(33 s_d). \tag{1}$$

Although H_{rms} predictions using Eq. (1) (henceforth γ predicted with Eq. (1) will be denoted as γ_{BS85}) are generally in good agreement with observations on planar (i.e., constant slope) beaches, model–data agreement for single-bar systems or for the innermost bar in multiple bar systems is usually less fair (e.g., Rivero et al., 1994; Southgate, 1995; Ruessink et al., 2001). Ruessink et al. (2001), for instance, found systematic H_{rms} overpredictions of up to 60% in the inner bar trough of the double-barred beach at Egmond aan Zee (Netherlands), but far better model–data agreement (without systematic overpredictions) in the outer bar trough. We realize that predictions of wave heights are generally good (even in multiple barred situations) in comparison with predictions of Q, radiation-stress related quantities (such as alongshore currents and undertow), and sediment transport (and thus morphological change). However, wave height predictions are usually the first step in morphodynamic process-based modelling, and errors in these predictions feed in directly to most subsequent computations. From this viewpoint, we feel that an improvement in wave height predictions on barred beaches is warranted.

Various attempts to improve H_{rms} predictions on non-planar beaches have been presented in the literature. One such attempt is the replacement of the clipped-Rayleigh distribution by a Rayleigh or Weibull distribution (e.g., Gerritsen, 1980; Roelvink, 1993; Baldock et al., 1998), as natural wave height distributions do not conform to a truncated distribution. However, the cross-shore evolution of H_{rms} in the surf zone is generally found to be rather insensitive to the choice of a particular distribution (Roelvink, 1993; Baldock et al., 1998). Only on steep slopes (>1:10) H_{rms} predictions based on the Rayleigh distribution (using γ_{BS85}) may outperform those based on the clipped-Rayleigh distribution (Baldock et al., 1998). A physics-based attempt has been to implement breaking-wave persistence in the Q formulation (Southgate and Wallace, 1994). These authors separated Q in a fraction of newly breaking waves and a fraction of breaking waves that persisted from seaward locations. The main purpose was to improve predictions of Q rather than wave heights. Another possible explanation for lower observed than modelled wave heights landward of bars is that it is a feature of the data analysis procedure. When surface elevation data is analysed spectrally, it is usual to truncate the analysed frequency range to exclude low frequencies. However, it is well known that the wave breaking process commonly involves transfer of energy from primary to low frequencies resulting in the generation of infragravity waves. This transfer of energy is not normally included in surf zone models (except when the main purpose is to model the generation of infragravity waves), so the modelled wave heights will tend to be larger than those measured in the field. However, this transfer of energy to low frequencies is a relatively small effect and would generally not be large enough to explain the observed discrepancies between measured and modelled wave heights landward of bars. In addition, this transfer of energy also occurs on planar beaches for which γ_{BS85} generally results in accurate H_{rms} predictions.

In this paper, we propose an empirical improvement to Battjes and Janssen (1978)-based cross-shore wave height modelling by implementing a new functional form for γ (i.e., other than Eq. (1)). The inverse modelling of the wave energy balance from detailed H_{rms} observations across a subtidal bar at Duck, NC, USA shows (Section 3) that γ is not a cross-shore constant but depends systematically on kh, where k is the local wave number. Verification against data from Egmond and Terschelling (Netherlands) subsequently shows that inner-trough H_{rms} predictions indeed improve and that outer-bar H_{rms} predications are about the same as those based on γ_{BS85} (Section 4). Additional verifications against laboratory wave data show the new empirical form for γ to be applicable to planar beaches as well (Section 5).

2. Model formulation

The applied model, a parametric model based on the wave energy balance, is the Battjes and Janssen (1978) wave transformation model in which, as proposed by

Baldock et al. (1998), the clipped-Rayleigh distribution is replaced by a Rayleigh distribution. For shore parallel depth contours, the energy balance reads

$$\frac{\mathrm{d}}{\mathrm{d}x}\left(\frac{1}{8}\rho g H_{\mathrm{rms}}^2 c_{\mathrm{g}} \cos\bar{\theta}\right) = -D, \tag{2}$$

where x is the cross-shore coordinate, positive onshore, ρ is the water density, g is the gravitational acceleration

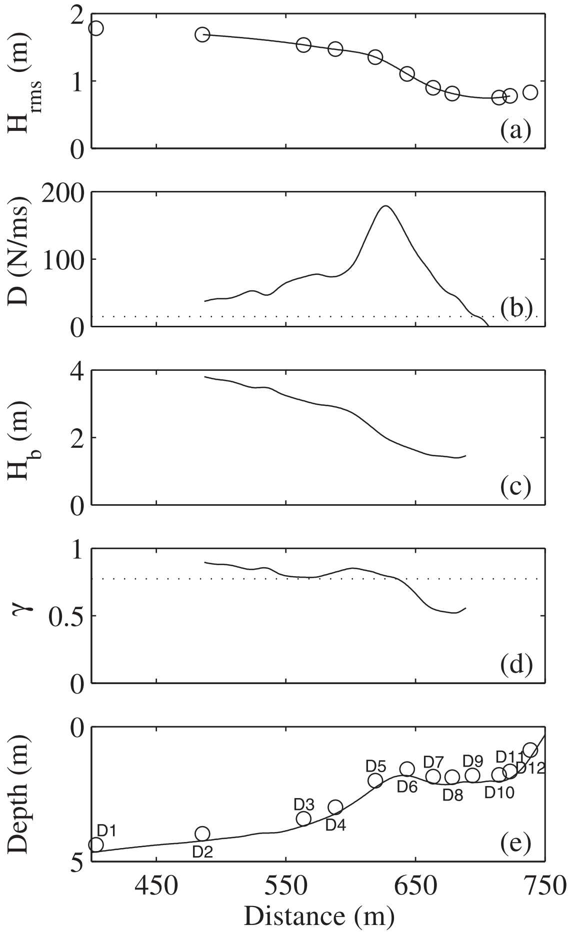

Fig. 1. Cross-shore distribution of (a) root-mean-square wave height H_{rms} (measured, circles; cubic spline, solid line), and inversely modelled (b) breaking-induced dissipation D, (c) maximum wave height H_{b}, and (d) breaking parameter γ, on September 22, 1994, 06:00 EST. (e) Depth relative to mean sea level on September 21, 1994 and instrument locations. The dotted line in (b) is the threshold $D = 15$ N/ms below which γ estimates were not retained. The dotted line in (d) is γ_{BS85}. Distance is relative to the offshore sensor in 8-m depth.

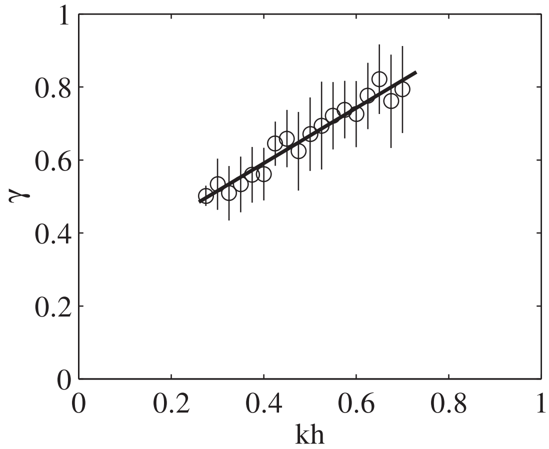

Fig. 2. Average (circles) and standard deviation (vertical bars) of γ versus kh based on all estimates with D>15 N/ms. The solid line is the least squares linear fit, Eq. (5).

and c_{g} is the group velocity evaluated at the representative wave period. Following Baldock et al. (1998), D is

$$D = \frac{\alpha}{4}\frac{1}{T_{\mathrm{p}}}\rho g \exp\left[-\left(\frac{H_{\mathrm{b}}}{H_{\mathrm{rms}}}\right)^2\right](H_{\mathrm{b}}^2 + H_{\mathrm{rms}}^2), \tag{3}$$

in which α is a proportionality constant of order one and H_{b} is the breaker height, given by Battjes and Janssen (1978)

$$H_{\mathrm{b}} = \frac{0.88}{k}\tanh\left(\frac{\gamma}{0.88}kh\right). \tag{4}$$

Here, k is the wave number of the representative period, h is the water depth ($= d + \zeta$, where d is depth and ζ is (tidal) water level with respect to mean sea level). Note that in the limit for deep water ($kh \rightarrow \infty$), Eq. (4) reduces to $H_{\mathrm{b}} = 0.88/k$, implying steepness-limited breaking, whereas in shallow ($kh \rightarrow 0$), Eq. (4) reduces

Table 1
Offshore wave conditions for H_{rms} verification data sets

Site	H_{rms} (m)	T_{p} (s)	$\bar{\theta}$ (deg)	N
Duck	0.29–2.19	4.5–7.0	− 30 to 50	270
Egmond	0.46–3.90	4.8–10.5	− 45 to 45	508
Terschelling	0.12–1.83	3.0–12.8	− 30 to 30	816

N: number of observations.

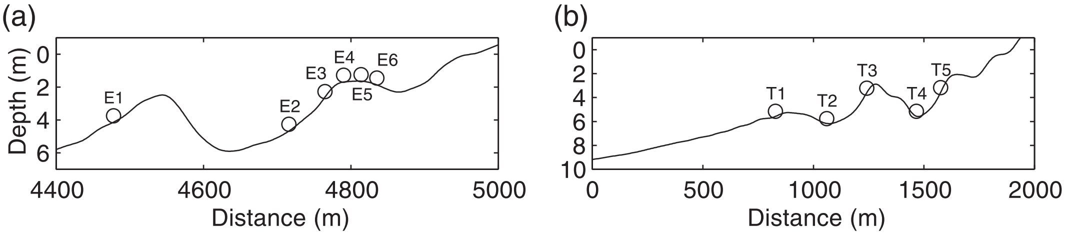

Fig. 3. Depth relative to mean sea level versus cross-shore distance and instrument locations at (a) Egmond on 19 October 1998 and (b) Terschelling in April 1994. Distance is relative to the location of the offshore sensor.

to $H_b = \gamma h$, corresponding to depth-limited breaking. Baldock et al. (1998) used γ_{BS85} as standard setting for γ. The wave model is solved here on a fourth-order Runge–Kutta scheme with adaptive step size control using the observed bathymetry, and offshore values of H_{rms}, T_p, $\bar{\theta}$ and ζ. Linear wave theory is used to calculate c_g and k, and Snell's law is used to determine $\bar{\theta}(x)$.

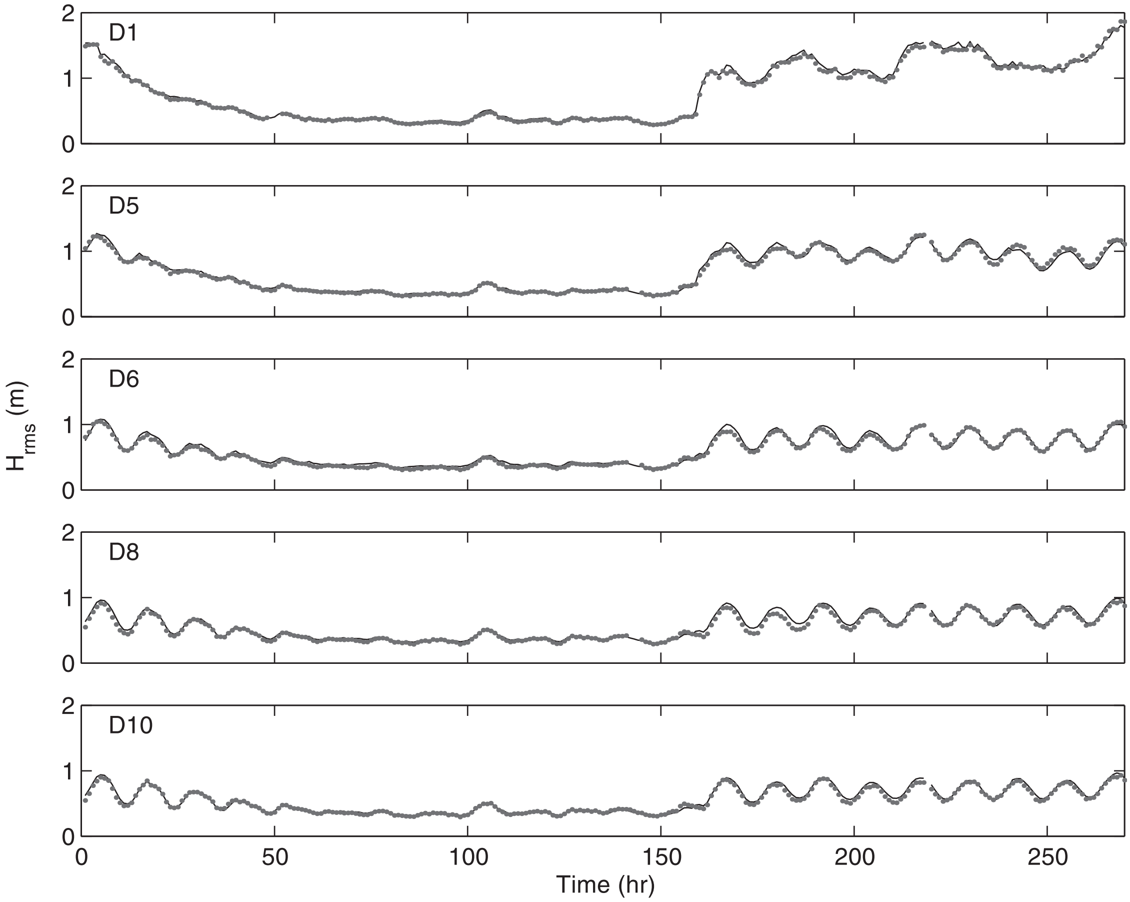

Fig. 4. Measured (symbols) and modelled (lines) H_{rms} from offshore (D1) to onshore (D10) versus time at Duck. For locations see Fig. 1e. Time = 0 corresponds to October 3, 1994, 12:00 EST.

3. Calibration

The calibration of the wave model is approached through an inverse modelling of Eqs. (2), (3) and (4) to yield the cross-shore distribution of γ. The basis of the inverse modelling is a spectrally derived H_{rms} data set collected during the Duck94 experiment at the U.S. Army Corps of Engineers Field Research Facility (FRF) (see, for example, Elgar et al., 1997; Gallagher et al., 1998; Feddersen et al. 1998). The data was obtained at up to 12 cross-shore positions, extending from the shore line across a subtidal bar to 4.5-m depth (Fig. 1). From the available data, an about 570-h portion (September 20, 1994–October 14, 1994) which spanned a wide range of conditions was selected, including both high-energy sea waves and low-energy swell, and for which depth profiles, surveyed with an amphibious vehicle, were regularly available. The first 300-h part (September 20, 1994–October 3, 1994) is used for calibration purposes; the remaining data is used for verification of the calibrated wave model. Offshore H_{rms} and T_p during the calibration part of the Duck94 campaign, estimated in 8-m water depth from a two-dimensional array of 15 bottom-mounted pressure sensors (Long, 1996), ranged from 0.12 to 1.98 m and 4.1 to 9.8 s, respectively. All H_{rms} at Duck, as well as all H_{rms} used later on in this paper, are based on spectral analysis rather than wave counting analysis.

Through each cross-shore transect of H_{rms}, a cubic spline was fitted to yield a smooth curve of H_{rms}

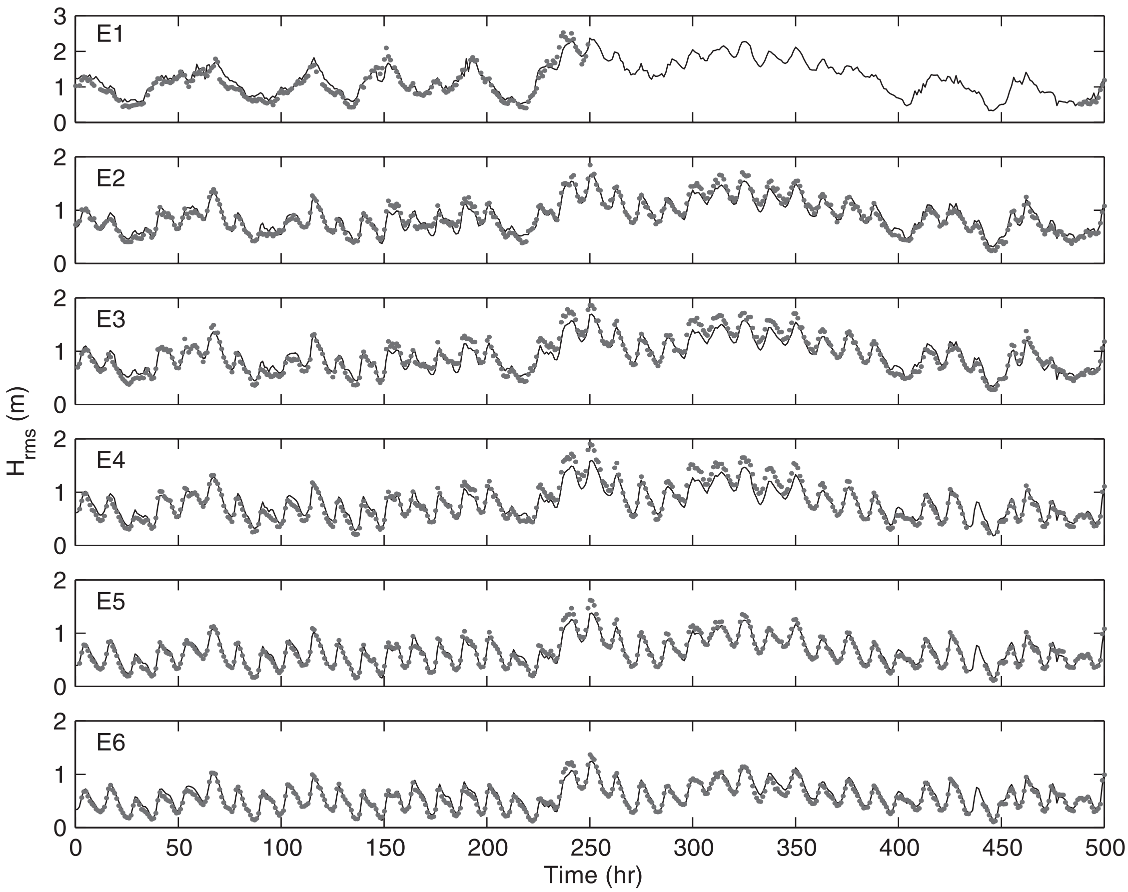

Fig. 5. Measured (symbols) and modelled (lines) H_{rms} from offshore (E1) to onshore (E6) versus time at Egmond. For locations, see Fig. 3a. Time = 0 corresponds to October 15, 1998, 09:00 MET.

transformation at a 1-m grid (e.g., Fig. 1a). Spline parts between the two most offshore (D1 and D2) and onshore (D11 and D12) sensors were not retained as the fitted H_{rms} transformations were often non-realistic. For each grid point, c_{g} and $\bar{\theta}$ were subsequently estimated using the offshore T_{p}, $\bar{\theta}$ and ζ, resulting in an estimate of the cross-shore evolution of the wave energy flux, $(1/8)\rho g c_{\mathrm{g}} H_{\mathrm{rms}}^2 \cos\bar{\theta}$. The cross-shore gradient of the wave energy flux equals the dissipation due to breaking D (Eq. (2), Fig. 1b). From D, the cross-shore evolution of H_{b} (Eq. (3), Fig. 1c) and subsequently, γ (Eq. (4), Fig. 1d) were computed, for which a non-linear fitting technique based on the Gauss–Newton method was adopted. To avoid spurious results, γ values based on $D < 15$ N/ms were discarded from further analysis. In total the selected calibration data resulted in about 5500 reliable γ estimates.

It is apparent from Fig. 1 that a cross-shore varying γ is needed to obtain accurate H_{rms} predictions. An attempt was made to relate γ to the local bed slope β (Sallenger and Holman, 1985; Thornton and Guza, 1986), $\beta/(kh)$ (Raubenheimer et al., 1996; Sénéchal et al., 2001), $\beta/(H_{\mathrm{rms}}/L)$ (Van Rijn and Wijnberg, 1996), and also to kh and H_{rms}/L separately, where $L = 2\pi/k$ and β was estimated from the observed depth profiles as the difference in vertical elevation over a distance L. The strongest correlation is the increase in γ with

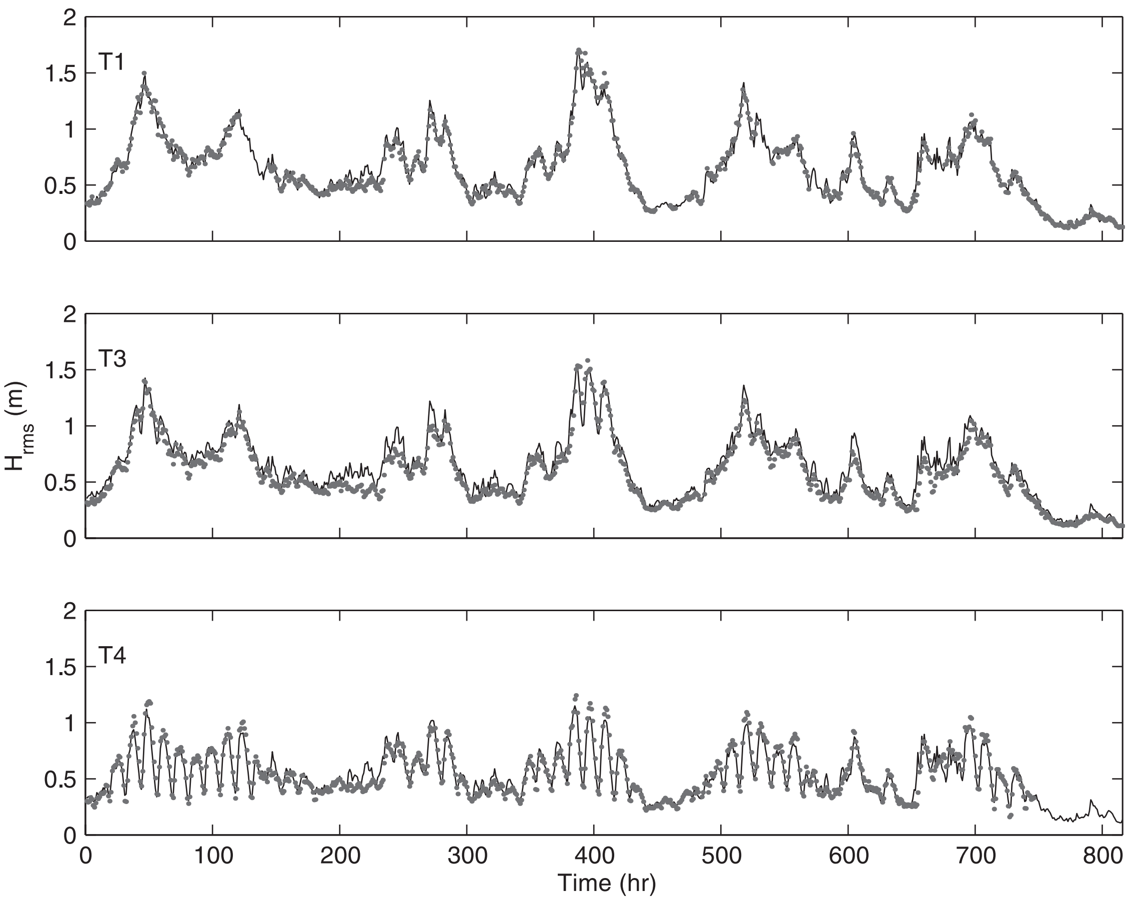

Fig. 6. Measured (symbols) and modelled (lines) H_{rms} from offshore (T1) to onshore (T4) versus time at Terschelling. For locations, see Fig. 3b. Time = 0 corresponds to May 25, 1994, 09:00 MET.

increasing kh (Fig. 2), with the least-squares linear fit given by

$$\gamma = 0.76kh + 0.29, \tag{5}$$

(correlation coefficient $r = 0.97$ for the kh range of $\approx 0.25-0.75$). Only a weak dependence of γ on β, $\beta/(kh)$, and $\beta/(H_{rms}/L)$ was observed ($|r| \leq 0.21$). Henceforth, we will denote γ estimated with Eq. (5) as γ_{var}. In shallow water, Eq. (5) corresponds to $\gamma_{var} \sim h^{0.5}$.

At this point, it is illustrative to discuss on which part of the cross-shore profile H_{rms} prediction will be affected most by the implementation of γ_{var} in Eq. (4). In 'deep' water, γ_{var} will be somewhat larger than γ_{BS85}, resulting, however, in comparable H_{rms} predictions. In some depths, γ_{var} and γ_{BS85} will be equal. This depth, denoted h_c, increases with increasing offshore H_{rms} and T_p. In depths shallower than h_c, γ_{var} will be less than γ_{BS85} and, as a consequence, H_{rms} decay with cross-shore distance will be larger. When, in multiple bar systems, h_c is found near the inner bar, H_{rms} predictions on outer bars are largely independent on whether γ_{var} or γ_{BS85} is used, but across the inner trough H_{rms} based on γ_{var} will be less than H_{rms} based on γ_{BS85}. This change in the cross-shore evolution of H_{rms} is qualitatively consistent with the observations (Section 1) that H_{rms} predictions in especially inner bar troughs need to be improved.

4. Field verification

The wave model with γ_{var} implemented in Eq. (4) was verified against three extensive H_{rms} data sets, collected at (1) the single-barred beach at Duck, (2) the double-barred beach at Egmond, Netherlands, and (3) the triple-barred beach at Terschelling, Netherlands. An overview of offshore wave conditions is presented in Table 1. Cross-shore profiles with instrumented locations at Egmond and Terschelling are shown in Fig. 3. Values of h_c indicate that the effect of γ_{var} on H_{rms} predictions will be most pronounced on and shoreward of the bar at Duck ($h_c \sim 2-5$ m) and on the inner bar and trough at Egmond ($h_c \sim 2-10$ m, but mostly <5 m). In contrast, no effect on H_{rms} predictions at Terschelling is anticipated ($h_c < 3$ m). The error reduction by the implementation of γ_{var} is quantified with the Brier Skill Score BSS (Murphy and Epstein, 1989)

$$\mathrm{BSS} = 1 - \frac{\mathrm{MSE}(H_{rms} \text{ with } \gamma_{var},\ \text{observed } H_{rms})}{\mathrm{MSE}(H_{rms} \text{ with } \gamma_{BS85}, \text{observed } H_{rms})}, \tag{6}$$

where MSE is the mean-square error, in general terms defined as $\mathrm{MSE}(x,y) = \langle (x-y)^2 \rangle$ with the angle brackets representing a time average. BSS is positive (negative) when the model accuracy using γ_{var} is

Table 2
Root-mean-square wave height error statistics

	r^2	ϵ_{rms} (m)	m	BSS
Duck				
D1	0.98	0.05	1.02	0.05
D2	0.98	0.04	1.01	0.49
D3	0.97	0.04	1.01	0.54
D4	no data			
D5	0.92	0.05	1.01	− 0.19
D6	0.94	0.04	1.03	0.61
D7	0.96	0.06	1.07	0.63
D8	0.94	0.05	1.06	0.63
D9	0.95	0.03	1.00	0.74
D10	0.96	0.04	1.04	0.72
D11	0.95	0.05	1.07	0.65
D12	0.87	0.04	1.01	0.68
Egmond				
E1	0.91	0.16	1.02	− 0.11
E2	0.92	0.09	0.98	− 0.03
E3	0.92	0.11	0.96	− 0.25
E4	0.93	0.12	0.95	− 0.01
E5	0.93	0.08	0.98	0.63
E6	0.92	0.07	1.03	0.77
Terschelling				
T1	0.98	0.05	1.00	0.07
T2	0.95	0.08	1.05	0.01
T3	0.95	0.09	1.08	− 0.05
T4	0.92	0.06	0.98	0.03
T5	0.95	0.09	1.12	0.09

ϵ_{rms} is the root-mean-square error between modelled and observed H_{rms}, r^2 and m are the correlation coefficient squared and the slope of the best-fit linear lines (forced through the origin) between modelled and observed H_{rms}. BSS is Brier Skill Score.
A value of $m>1$ corresponds to model overprediction of observed H_{rms}. Values at Duck exclude results for hours 40–160 during which waves did not break across the instrument array (see Fig. 4).

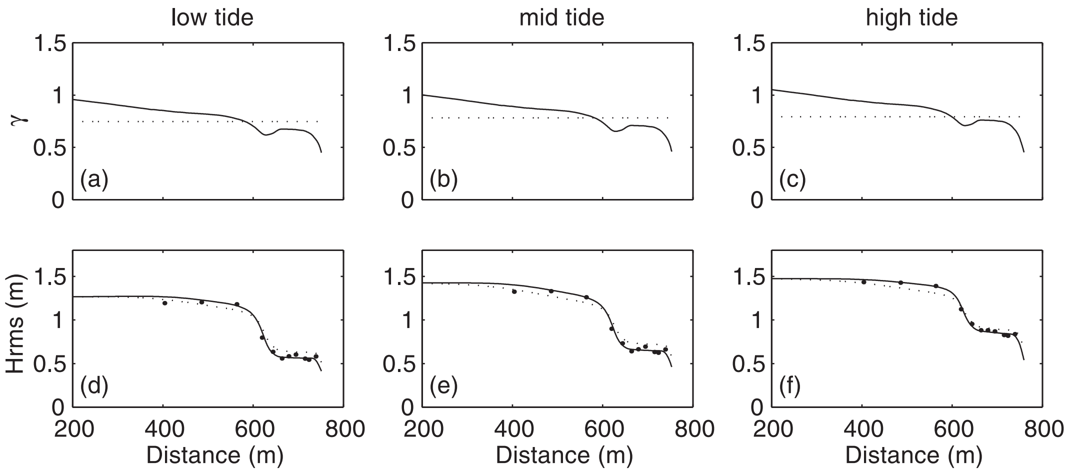

Fig. 7. Modelled (a)–(c) breaker parameter γ and (d)–(f) root-mean-square wave height H_{rms} versus cross-shore distance at Duck. Solid (dotted) lines are model results with γ_{var} (γ_{BS85}). Dots in (d)–(f) are measured H_{rms}. Columns from left to right: low tide (t=236 h), mid tide (t=234 h), high tide (t=229 h). The bar crest is located at x=630 m.

greater (less) than the accuracy using γ_{BS85}. BSS multiplied by 100 is a measure of percentage improvement in accuracy. Details on data acquisition and processing are given in Ruessink et al. (2001) for Egmond and in Ruessink et al. (1998) and Houwman (2000) for Terschelling.

The wave model with γ_{var} yields accurate H_{rms} predictions across the entire profile (Figs. 4–6) with skill $r^2 \geq 0.87$ at all sensors (Table 2). Observed and predicted H_{rms} show the transition from H_{rms} that are closely related to offshore H_{rms} to tidally modulated H_{rms} at the shoreward sensors (Figs. 4–6). Root-mean-square errors ϵ_{rms} for individual sensors vary from 0.03 to 0.16 m (Table 2), with differences between the site being related to the different energetic conditions. Average ϵ_{rms} are 0.05, 0.10 and 0.07

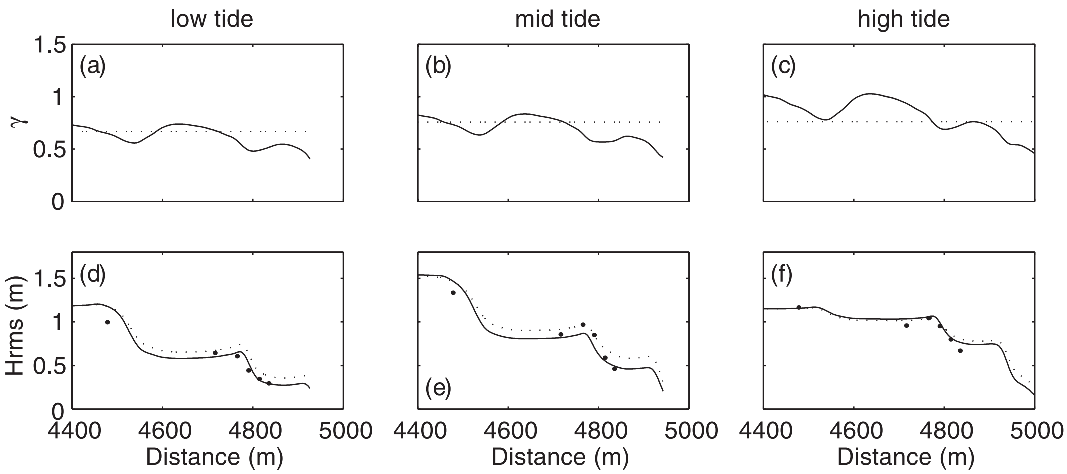

Fig. 8. Modelled (a)–(c) breaker parameter γ and (d)–(f) root-mean-square wave height H_{rms} versus cross-shore distance at Egmond. Solid (dotted) lines are model results with γ_{var} (γ_{BS85}). Dots in (d)–(f) are measured H_{rms}. Columns from left to right: low tide (t=76 h), mid tide (t=52 h), high tide (t=56 h), see also Fig. 6 in Ruessink et al. (2001). The outer and inner bar crests are located at x=4540 and 4800 m, respectively.

m for Duck, Egmond and Terschelling, respectively. Slopes m of best-fit linear lines (forced through the origin) between observed and predicted H_{rms} are close to 1 at all sensors (Table 2). BSS values imply a 50–80% improvement in accuracy (Table 2) in the bar trough at Duck (D7–D10) and inner bar-trough at Egmond (E5–E6), where prediction errors using γ_{BS85} were largest (Ruessink et al., 2001). As expected from the aforementioned h_c values, γ_{var} and γ_{BS85} result in the same predictive skill (i.e., BSS ≈ 0) at the outer bar at Egmond (E1) and at all Terschelling sensors (Table 2). We cannot, however, assign much significance to the Duck results since data for these results are from the same site as the data for the γ calibration. Although different data sets from Duck were used for calibration and verification, we would expect a much stronger correlation between the two Duck data sets than between one Duck data set and a data set from another site. The evidence in favour of γ_{var} therefore comes mainly from the Egmond and Terschelling data. Examples of the predicted cross-shore distribution of γ and H_{rms} at low, mid and high tide are shown in Figs. 7 and 8 for Duck and Egmond, respectively.

5. Discussion

In this paper, a new functional form for the breaking-wave parameter γ in Battjes and Janssen (1978)-type parametric wave transformations models was derived empirically through an inverse modelling of a high-resolution (in the cross-shore) H_{rms} data set collected across a subtidal bar at Duck, NC. This new form, a local dependence of γ on kh (Fig. 2, Eq. (5)), results in H_{rms} predictions that are in better agreement with measured H_{rms} than predictions based on the commonly applied parameterization of Battjes and Stive (1985). Particularly, the predicted stronger H_{rms} decay across inner bars causes an up to 80% improvement in model accuracy in inner bar troughs.

Although our work was motivated by the need to improve H_{rms} predictions in the inner bar-trough zone, we would obviously like to see that γ_{var} does not deteriorate H_{rms} predictions in cases for which γ_{BS85} does show good predictive skill, most notably, on planar beaches. To this end, the wave model was additionally run for 11 small-scale, plane-sloping laboratory tests (Table 3, note that Battjes and Stive (1985) used tests 1, 2, 3, 6 and 7 to derive γ_{BS85}). As can be deduced from Fig. 9 and from the error statistics computed for each test using observed and predicted H_{rms} at all measurement points (Table 3), γ_{var} results in about the same or slightly improved H_{rms} predictions (in most cases, BSS>0), implying that γ_{var}, although derived from data collected on a barred beach, is also applicable to planar beaches.

The trend in γ_{var} variation with kh and the absence of a β dependence of γ_{var} contrasts with field observations of the height-to-depth ratio (Raubenheimer et al., 1996; Sénéchal et al., 2001) and model computations based on the one-dimensional depth-averaged non-linear shallow water equations (Raubenheimer et al., 1996). These studies find a positive

Table 3
Laboratory experiments and H_{rms} error statistics

No.	Source	Code	H_{rms} (m)	T_p (s)	N	β	r^2	ϵ_{rms} (m)	m	BSS
1	Battjes and Janssen (1978)	BJ2	0.144	1.84	6	1:20	0.99	0.0038	0.99	0.52
2	Battjes and Janssen (1978)	BJ3	0.121	2.48	8	1:20	0.99	0.0028	1.01	0.80
3	Battjes and Janssen (1978)	BJ4	0.142	2.16	8	1:20	0.99	0.0028	0.99	0.85
4	Thompson and Vincent (1984)	–	0.044	2.50	9	1:30	0.98	0.0023	1.02	0.63
5	Thompson and Vincent (1984)	–	0.056	1.25	9	1:30	0.94	0.0028	1.02	0.18
6	Stive (1985)	MS10	0.142	2.93	22	1:40	0.57	0.0206	0.92	– 0.36
7	Stive (1985)	MS40	0.135	1.58	24	1:40	0.97	0.0086	0.97	– 0.21
8	Baldock and Huntley (2002)	J1033C	0.048	1.00	35	1:10	0.99	0.0016	1.02	0.31
9	Baldock and Huntley (2002)	J6033A	0.100	1.67	35	1:10	0.97	0.0046	1.02	0.51
10	Baldock and Huntley (2002)	J6033B	0.075	1.67	35	1:10	0.94	0.0042	1.02	0.37
11	Baldock and Huntley (2002)	J6033C	0.050	1.67	35	1:10	0.70	0.0035	1.02	0.24

N = number of cross-shore measurement points, not including the offshore boundary.

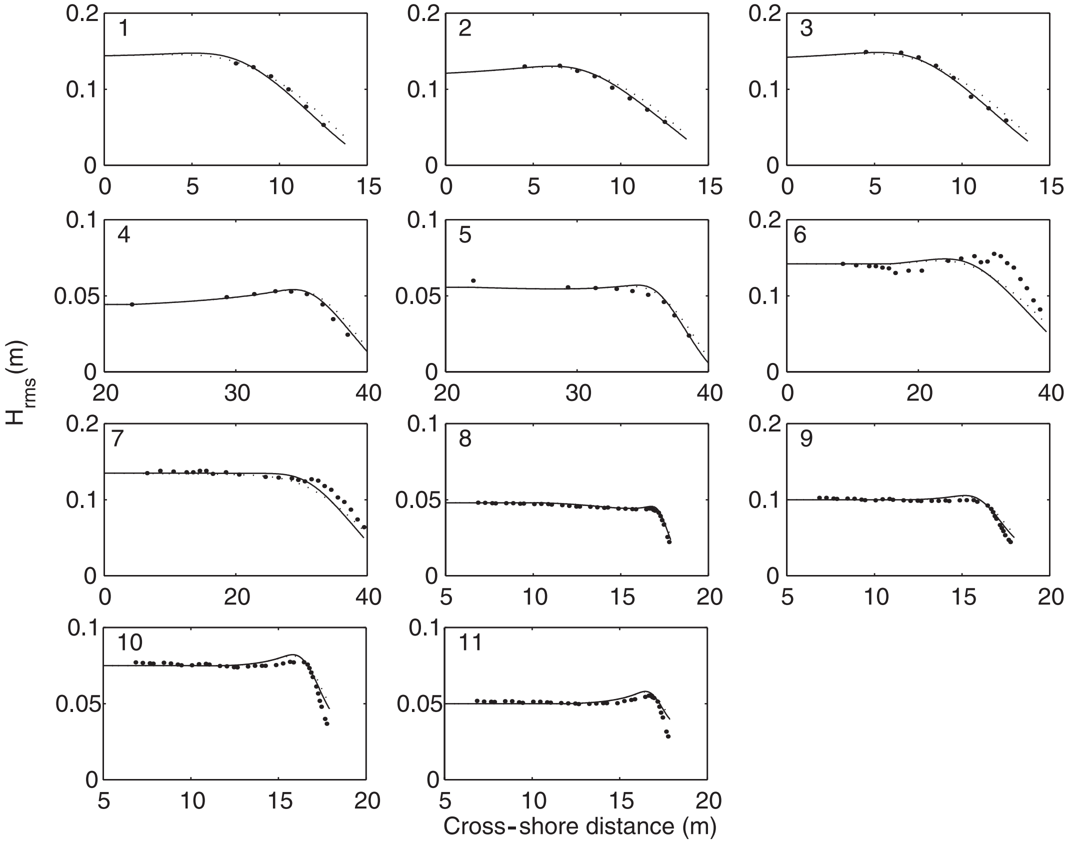

Fig. 9. Modelled (solid line: γ_{var}; dotted line: γ_{BS85}) and measured (symbols) H_{rms} versus cross-shore distance for the 11 planar-beach laboratory cases listed in Table 3.

linear dependence of γ on $\beta/(kh)$, although the slope and intercept of the best-fit linear line differ considerably between Raubenheimer et al. (1996) and Sénéchal et al. (2001). It is stressed that, although both parameters are referred to as γ and are height-to-depth ratios, they are not the same. In the Battjes and Janssen (1978) model γ is related to the maximum wave height H_b and is prescribed empirically, whereas in the field or in Raubenheimer et al.'s model γ is defined as H_{rms}/h based on physical arguments. In addition, a constant α value was applied in Eq. (3); as already suggested by Battjes and Stive (1985), deviations from this constant value are accounted for empirically in γ. Thus, our γ_{var} cannot be compared directly to observed height-to-depth ratios and is best interpreted as the optimum setting of the free model parameter γ. We do not know of any physical mechanism why γ_{var} should have a positive dependence on local kh and should lack a dependence on β.

6. Conclusions

Our inverse modelling results show that that the free model parameter γ in the Battjes and Janssen (1978) wave model is a locally varying parameter that increases linearly with the product of the local wavenumber and waterdepth kh (i.e., Eq. (5)). This contrasts with the present-day implemented functional form of a cross-shore constant γ depending weakly on the offshore wave steepness (Battjes and Stive, 1985). Implementation of the locally varying γ improves H_{rms} predictions by up to 80%, particularly across inner bar-troughs, where errors using the cross-shore constant γ are largest. The proposed new functional form of

γ also results in accurate H_{rms} predictions on planar beaches.

Acknowledgements

This work was carried out as part of the Delft Cluster project Coasts under number 03.01.03. D.J.R. Walstra was partly supported by the Dutch Rijksinstituut voor Kust en Zee through VOP-project Z3412. We thank Steve Elgar, R.T. Guza and Falk Feddersen for providing the data for Duck, and Tom Baldock for providing the data for laboratory tests 8–11. The Egmond and Terschelling data were collected in the framework of the Coast3D and Nourtec projects, funded by the European Commission's research program MAST under contract MAS3-CT97-0086 and MAS2-CT93-0049, respectively.

References

Baldock, T.E., Huntley, D.A., 2002. Long wave forcing by the breaking of random waves on a beach. Proc. R. Soc. Lond. A 258, 2177–2202.

Baldock, T.E., Holmes, P., Bunker, S., Van Weert, P., 1998. Cross-shore hydrodynamics within an unsaturated surf zone. Coast. Eng. 34, 173–196.

Battjes, J.A., Janssen, J.P.F.M., 1978. Energy loss and set-up due to breaking of random waves. Proc. 16th Int. Conf. on Coastal Engineering. ASCE, New York, pp. 570–587.

Battjes, J.A., Stive, M.J.F., 1985. Calibration and verification of a dissipation model for random breaking waves. J. Geophys. Res. 90, 9159–9167.

Elgar, S., Guza, R.T., Raubenheimer, B., Herbers, T.H.C., Gallagher, E., 1997. Spectral evolution of shoaling and breaking waves on a barred beach. J. Geophys. Res. 102, 15797–15805.

Feddersen, F., Guza, R.T., Elgar, S., Herbers, T.H.C., 1998. Alongshore momentum balances in the nearshore. J. Geophys. Res. 103, 15667–15676.

Gallagher, E.L., Elgar, S., Guza, R.T., 1998. Observations of sand bar evolution on a natural beach. J. Geophys. Res. 103, 3203–3215.

Gerritsen, F., 1980. Wave attenuation and wave set-up on a coastal reef. Proc. 17th Int. Conf. on Coastal Eng. ASCE, New York, pp. 444–461.

Houwman, K.T., 2000. Tide, wind- and wave-driven flow processes in the nearshore zone. PhD thesis, Dept. of Physical Geography, Utrecht University, Netherlands.

Long, C.E., 1996. Index and bulk parameters for frequency–direction spectra measured at CERC Field Research Facility, June 1994 to August 1995. Misc. Pap. CERC-96-6, U.S. Army Eng. Waterw. Exp. Stn., Vicksburg, MS.

Murphy, A.H., Epstein, E.S., 1989. Skill scores and correlation coefficients in model verification. Mon. Weather Rev. 117, 572–581.

Raubenheimer, B., Guza, R.T., Elgar, S., 1996. Wave transformation across the inner surf zone. J. Geophys. Res. 101, 25589–25597.

Rivero, F.J., Sánchez-Arcilla, A., Beyer, D., 1994. Comparison of a wave transformation model with LIP-IID data. Proc. Coastal Dynamics '94. ASCE, New York, pp. 518–532.

Roelvink, J.A., 1993. Dissipation in random wave groups incident on a beach. Coast. Eng. 19, 127–150.

Ruessink, B.G., Houwman, K.T., Hoekstra, P., 1998. The systematic contribution of transporting mechanisms to the cross-shore sediment transport in water depths of 3 to 9 m. Mar. Geol. 152, 295–324.

Ruessink, B.G., Miles, J.R., Feddersen, F., Guza, R.T., Elgar, S., 2001. Modeling the alongshore current on barred beaches. J. Geophys. Res. 106, 22451–22463.

Sallenger, A.H., Holman, R.A., 1985. Wave-energy saturation on a natural beach of variable slope. J. Geophys. Res. 90, 11939–11944.

Sénéchal, N., Dupuis, H., Bonneton, P., Howa, H., Pedreros, R., 2001. Observation of irregular wave transformation in the surf zone over a gently sloping sandy beach on the French Atlantic coastline. Oceanol. Acta 24, 545–556.

Southgate, H.N., 1995. Prediction of wave breaking processes at the coastline. In: Rahman, M. (Ed.), Advances in Fluid Mechanics, vol. 6. Computational Mechanics Publications, Southampton, UK.

Southgate, H.N., Wallace, H.M., 1994. Breaking wave persistence in parametric surf zone models. Proc. Coastal Dynamics '94. ASCE, New York, pp. 543–555.

Stive, M.J.F., 1985. A scale comparison of wave breaking on a beach. Coast. Eng. 9, 151–158.

Thompson, E.F., Vincent, C.L., 1984. Shallow water wave height parameters. J. Waterw., Port, Coast. Ocean Eng. 119, 293–298.

Thornton, E.B., Guza, R.T., 1986. Surf zone longshore currents and random waves: field data and models. J. Phys. Oceanogr. 16, 1165–1178.

Van Rijn, L.C., Wijnberg, K.M., 1996. One-dimensional modelling of individual waves and wave-induced longshore currents in the surf zone. Coast. Eng. 28, 121–145.